



European Union's Seventh Framework Programme

Grant Agreement №: **603521**

Project Acronym: **PREFACE**

Project full title: **Enhancing prediction of tropical Atlantic climate and its impacts**

Instrument: Collaborative Project

Theme: ENV.2013.6.1-1 – *Climate-related ocean processes and combined impacts of multiple stressors on the marine environment*

Start date of project: 1 November 2013

Duration: 48 Months

**Deliverable reference number and full title:** *D11.2: Impact of model improvements on climate projections*

**Lead beneficiary for this deliverable:** UiB & UniRes

**Due date of deliverable:** 31.01.2018

**Actual submission date:** 02.02.2018

Project co-funded by the European Commission within the Seven Framework Programme (2007-2013)		
Dissemination Level		
<b>PU</b>	Public	X
<b>PP</b>	Restricted to other programme participants (including the Commission Services)	
<b>RE</b>	Restricted to a group specified by the Consortium (including the Commission Services)	
<b>CO</b>	Confidential, only for members of the Consortium (including the Commission Services)	

*If this report is not to be made public, please state here why:*

**Contribution to project objectives** – with this deliverable, the project has contributed to the achievement of the following objectives (from Annex I / DOW, Section B1.1.):

N.º	Objective	Yes	No
1	Reduce uncertainties in our knowledge of the functioning of Tropical Atlantic (TA) climate, particularly climate-related ocean processes (including stratification) and dynamics, coupled ocean, atmosphere, and land interactions; and internal and externally forced climate variability.	x	
2	Better understand the impact of model systematic error and its reduction on seasonal-to-decadal climate predictions and on climate change projections.	x	
3	Improve the simulation and prediction TA climate on seasonal and longer time scales, and contribute to better quantification of climate change impacts in the region.	x	
4	Improve understanding of the cumulative effects of the multiple stressors of climate variability, greenhouse-gas induced climate change (including warming and deoxygenation), and fisheries on marine ecosystems, functional diversity, and ecosystem services (e.g., fisheries) in the TA.	x	
5	Assess the socio-economic vulnerabilities and evaluate the resilience of the welfare of West African fishing communities to climate-driven ecosystem shifts and global markets.		x

**Author(s) of this deliverable:** Shunya Koseki (UiB), Noel Keenlyside (UiB), Markus Jochem (UPCH), Anna-Lena Deppenmeier (WU), Aurore Voldoire (MF-CNRM), Emilia Sanchez-Gomez (CERFACS), Marta Martín-Rey (CERFACS)

**Deviation from planned efforts for this deliverable:** None to our best knowledge

### Report

#### **Executive Summary**

This report is Deliverable 11.2 of PREFACE project, contributed by the work package WP11. A main task of WP11 is to investigate impacts of model improvement and systematic error reduction in climate prediction and projection. In particular, this Deliverable focuses on the climate projection with multiple CGCMs and with several approaches for model improvement.

UiB and UniRes developed an alternative method of anomaly coupling and implemented it to the Norwegian CGCM (NorESM). The anomaly coupling successfully reduces the tropical climatological biases of sea surface temperature (SST) and precipitation. Their climate projection experiment shows that the warming of tropical Atlantic is more sensitive to the global warming effect under reduced model's systematic error. In particular, they found that the SST in the Gulf of Guinea is relatively warmer in the experiment with the anomaly coupling than in the experiment without the anomaly coupling. Correspondingly, the tropical Atlantic ITCZ shifts more southward under the global warming with the anomaly coupling. UCPH developed a new parameterization of ocean mixing layer and implemented it to the same CGCM. This parameterization also improves the current tropical climate state. They also found that the warming tendency in the tropical Atlantic is higher and the ITCZ shifts southward with the new parameterization under the global warming. These results are consistent and we can suggest that a better-climatology model is more sensitive to the global warming in the tropical Atlantic Ocean.

WU improved a parameterization of ocean mixing layer for European CGCM (EC-Earth), leading to reduce the bias, demonstrated in climate projection experiments. They focus on the remarkable

modes of Atlantic variability and found that new parameterization influences such the long-term variability. A part of this work is now under preparation for publication.

Additionally, WU, UiB, and UniRes have now shared the data of their climate change experiments with other work packages, WP12 and WP13.

CERFACS and MF-CNRM collaboratively developed a new version of the French CGCM (CNRM-CM) and performed a climate projection with old and new versions of the CGCM. They also focus on the Atlantic variability modes and their future modulation. Their new version of CGCM shows higher sensitivity of SST warming in the tropical Atlantic and corresponding ITCZ modification. On the other hand, the Atlantic Meridional and Zonal Modes of variability are less sensitive to the global warming in the new version of the CGCM than in the old version. They will continue to investigate what causes the lower sensitivity of the tropical Atlantic variability mode to global warming.

Additionally, CERFACS investigated the inter-basin teleconnection between the tropical Atlantic and Pacific Oceans under global warming with their previous version of CGCM. They found that the ENSO-forced diabatic source shifts more eastward and can influence the North Atlantic variability under global warming. This causes the reduction of trade winds over the tropical Atlantic linking with the weakening of the South Atlantic Anticyclone. They concluded that the inter-basin teleconnection becomes stronger under the global warming due to intensified ENSO variability and more active ocean dynamics in the tropical Atlantic.

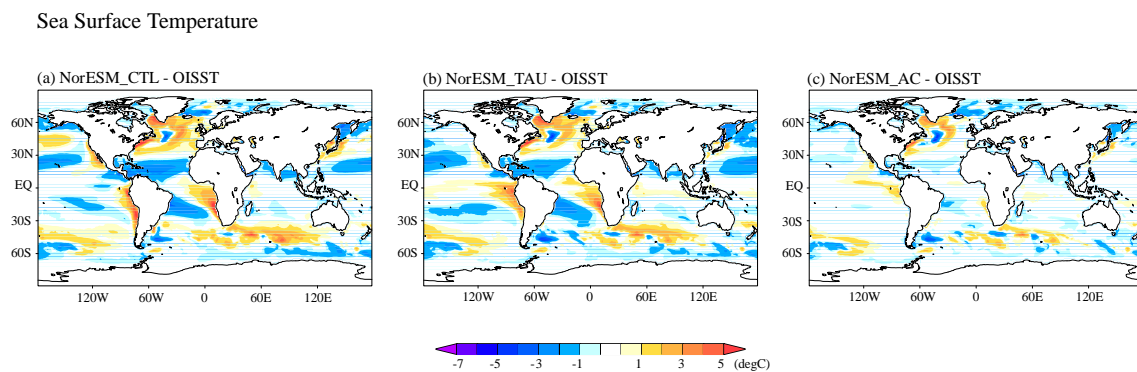
## 1. Impact of an anomaly coupling and new parameterization with NorESM

Demissie, T. (UniRes) ; Keenlyside, N. (UiB) ; Koseki, S., (UiB) ; Bethke, I., (UniRes); Pillar H (UCPH); Jochum M. (UCPH); Nuterman R. (UCPH)

Large climatological bias is a common issue in CGCMs. With such biased simulation, it is unclear how robust are future climate projections. Therefore, this study implement separately two methodologies to suppress the model biases of climatological mean state, an anomaly coupling and an improved ocean mixing layer scheme, and investigate how the bias-adjusted climate projection is different from standard experiment of climate projection. In the experiments with the two methods, the SST in the tropical Atlantic is more sensitive to the global warming and in particular, the SST in the Gulf of Guinea is much warmer in the bias-corrected experiments than in the standard experiments. Correspondingly, the position of the Atlantic ITCZ shifts more southward. These results indicate that the climate projections depend strongly on the simulated climate mean state.

### A- An alternative anomaly coupling:

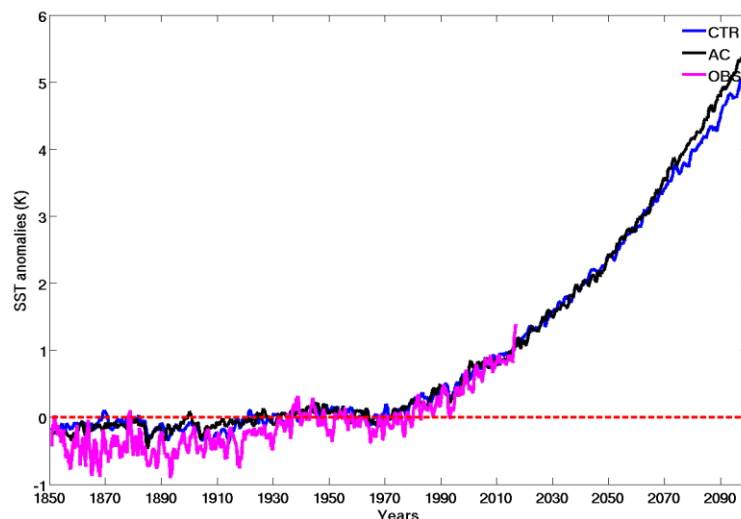
UniRes and UiB have developed an alternative anomaly coupling methodology (Toniazzi and Koseki, submitted). BY this methodology, momentum flux and sea surface temperature (SST) is corrected by the observed values and it is successful to reduce the SST and associated precipitation biases, in particular, in the tropical oceans (Fig.1.1).



**Figure 1.1: Annual-mean climatological bias of SST for (a) free run, (b) experiment of wind stress replacement, and (c) experiment of wind stress and SST replacement (anomaly coupling).**

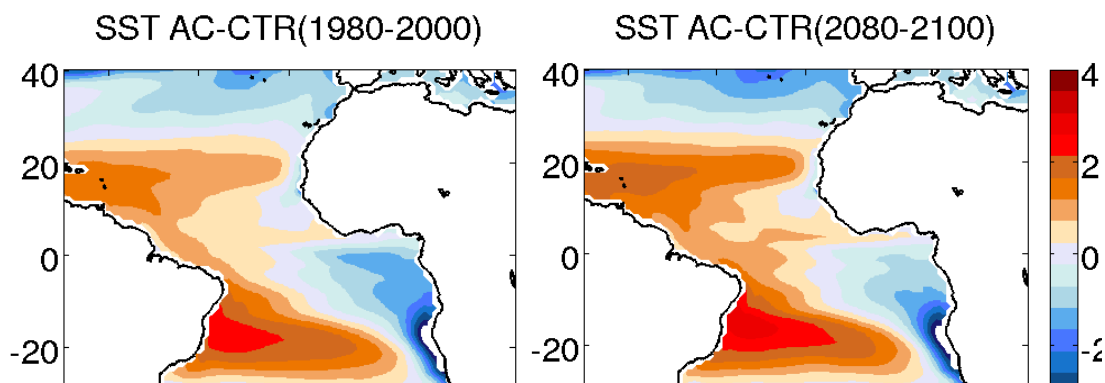
### B- Climate projection experiment with the anomaly coupling:

We conduct a numerical experiment of NorESM without and with the anomaly coupling. Both experiments are span-up from 1850 under pre-industrial conditions to 2099 with the emissions of RCP8.5 scenario. For the anomaly coupling, the HadISST and ERA-Interim monthly climatology for 1980-2000 are replaced by the converged model climatology of NorESM free run (Toniazzi and Koseki, submitted). In this study, it is assumed that the model's systematic bias with respect to the observation is unchanged for the future simulation.



**Figure 1.2 : Time series of global-mean SST for observation (magenta), NorESM free run (blue) and NorESM with the anomaly coupling (black).**

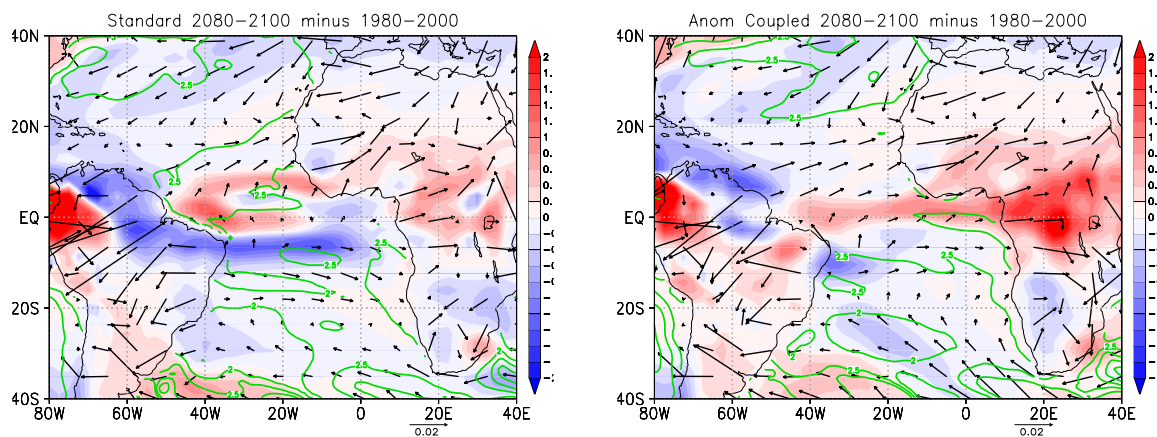
Figure 1.2 presents a time series of global-mean SST for observation and two NorESM experiments. Generally, NorESM can reproduce the global warming response in the latter 20th century to the beginning of the 21st century. Curiously, the hiatus between 2000-2010 seems to be also represented to some extent by NorESM simulations. Under the RCM8.5 scenario, the global warming continues and the increment of the global-mean temperature is enhanced up to 5K at the end of 21st century. It is worth noting that NorESM with the anomaly coupling shows relatively larger warming from 2070 to 2099. It indicates that the bias-corrected CGCM is more sensitive to the global-warming.



**Figure 1.3: Annual mean SST difference between 2080-2099 and 1980-2000 for (left) NorESM free run and (right) NorESM with the anomaly coupling.**

Figure 1.3 gives a horizontal map of annual-mean SST difference between 2080-2099 and 1980-2000 in the tropical Atlantic Ocean. In NorESM free run, the tropical Atlantic warms everywhere and the equatorial Atlantic experiences by about a 2K warming for 100 years. On the other hand, the warming in the subtropical Atlantic Ocean is moderate. With the anomaly coupling, the warming in the equatorial Atlantic Ocean is highly enhanced (up to 3K) and the warming in the subtropics is

almost identical with that of NorESM free run (the higher sensitivity is found in the tropics).



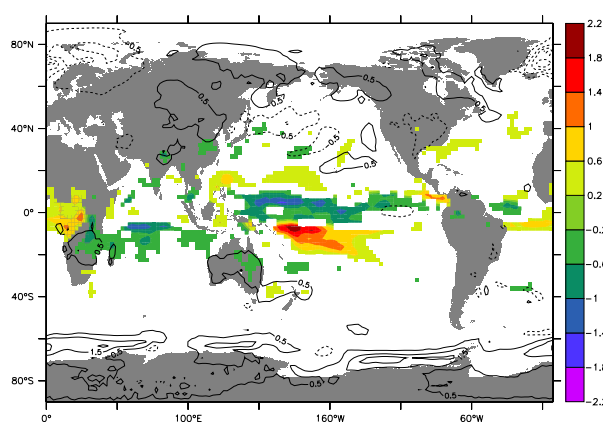
**Figure 1.4: Annual mean precipitation (colour), wind stress (vector) differences between 2080-2099 and 1980-2000 for (left) NorESM free run and (right) NorESM with the anomaly coupling.**

Figure 1.4 gives a horizontal map of annual-mean difference in the atmospheric variables between 2080-2099 and 1980-2000 in the tropical Atlantic Ocean. The most remarkable difference between two experiments is the rainfall band over the equatorial Atlantic: In NorESM free run, the equatorial rainband is partially reinforced in the west. On the other hand, the equatorial rainband is entirely strengthened, which is attributed to the enhanced warmed SST as seen in Fig. 1.3. Correspondingly, the easterly trade winds are weakened in NorESM with the anomaly coupling.

Koseki et al. (in prep) shows that the climatological mean state can modify the equatorial air-sea interaction responsible for the inter-annual variability. It can be expected that the behaviour of the inter-annual variability will be also modified more sensitively with the anomaly coupling.

#### C- Climate projection experiment with a new parameterization of ocean mixing dynamics:

Pillar et al. (in prep) have developed a new parameterization of inertial ocean mixing dynamics, which leads to a major improvement for present day climate simulation. We demonstrate climate projection experiments of NorESM without (NorESM\_CTL)/with (NorESM\_NIW) the new parameterization under a condition of RCP8.5 scenario.



**Figure 1.5: Trend difference in precipitation (colour) and SST (contour) between NorESM\_NIW and NorESM\_CTL.**

Figure 1.5 gives a trend difference in precipitation and SST in NorESM\_NIW and NorESM\_CTL. Interestingly, the equatorial precipitation tends to be enhanced and reduced in the south and north of the equator over the Pacific and Atlantic Ocean in NorESM\_NIW. This indicates that the position of Inter-tropical Convergence Zone (ITCZ) shifts more southward. This shift is not seen over the Indian Ocean. Rather, the precipitation over the Southern Indian Ocean is reduced in NorESM\_NIW. Focusing on the tropical Atlantic, NorESM\_NIW also shows the warmer SST in the tropical Atlantic under RCP8.5 scenario and this causes the southern shift of the ITCZ.

## 2. A new parameterization with EC-Earth

Deppenmeier, A. L. (WU)

We have performed sensitivity experiments with a coupled single column version of EC-Earth, consisting of IFS (cycle 40r1), Nemo3.6, and OASIS3 (Hartung et al 2018). The results show that vertical mixing in the upper ocean strongly decreases with little added temperature stratification and is unlikely to recover (over the course of 10day, there is a warm layer forming at the top of the mixed layer leading to weakening the mixing). The decreased ocean vertical mixing then allows the sea surface temperature to warm strongly, without cold waters being mixed up to the surface. Based on these findings Wageningen University has completed a climate projection run from 1950-2100 with improved parametrisation in the ocean vertical mixing scheme (TKE). A historical as well as a transient control experiment have been run in order to compare to the new parametrisation.

After fifty years of runtime the warm bias in the tropical Atlantic is strongly reduced in comparison to the control transient run (Fig. 2.1).

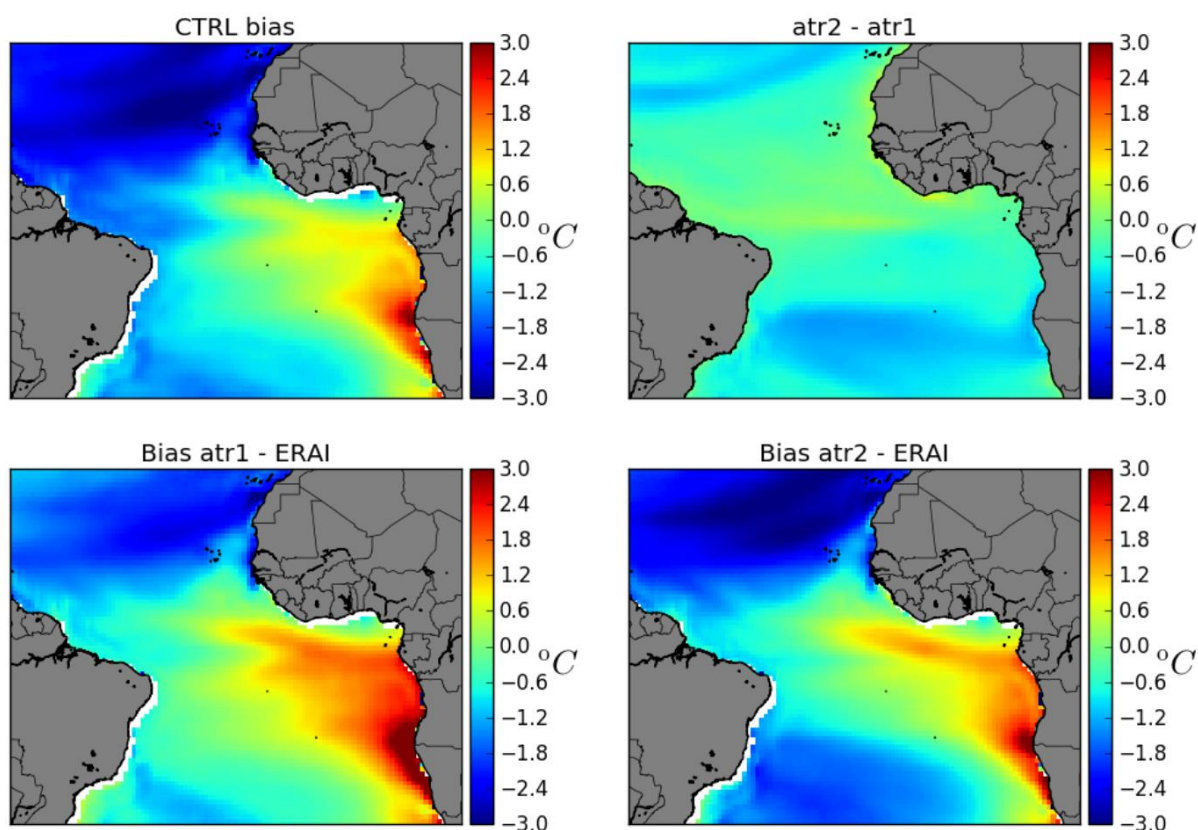


Figure 2.1: Yearly averaged SST bias between 2000-2009 with respect to ERA-Interim.

In current climate we observe a meridional and a zonal mode in the tropical Atlantic. To see how these behave under changing climate with the standard as well as the improved model we have performed EOF analysis of the SST modes in the future (2070-2079). In both transient runs there is a zonal mode (EOF1) and a meridional mode (EOF2) present. The former changes in future climate (Fig. 2.1).

We have shared data from our simulations with WP12/13 to assess the impact of the improved model.

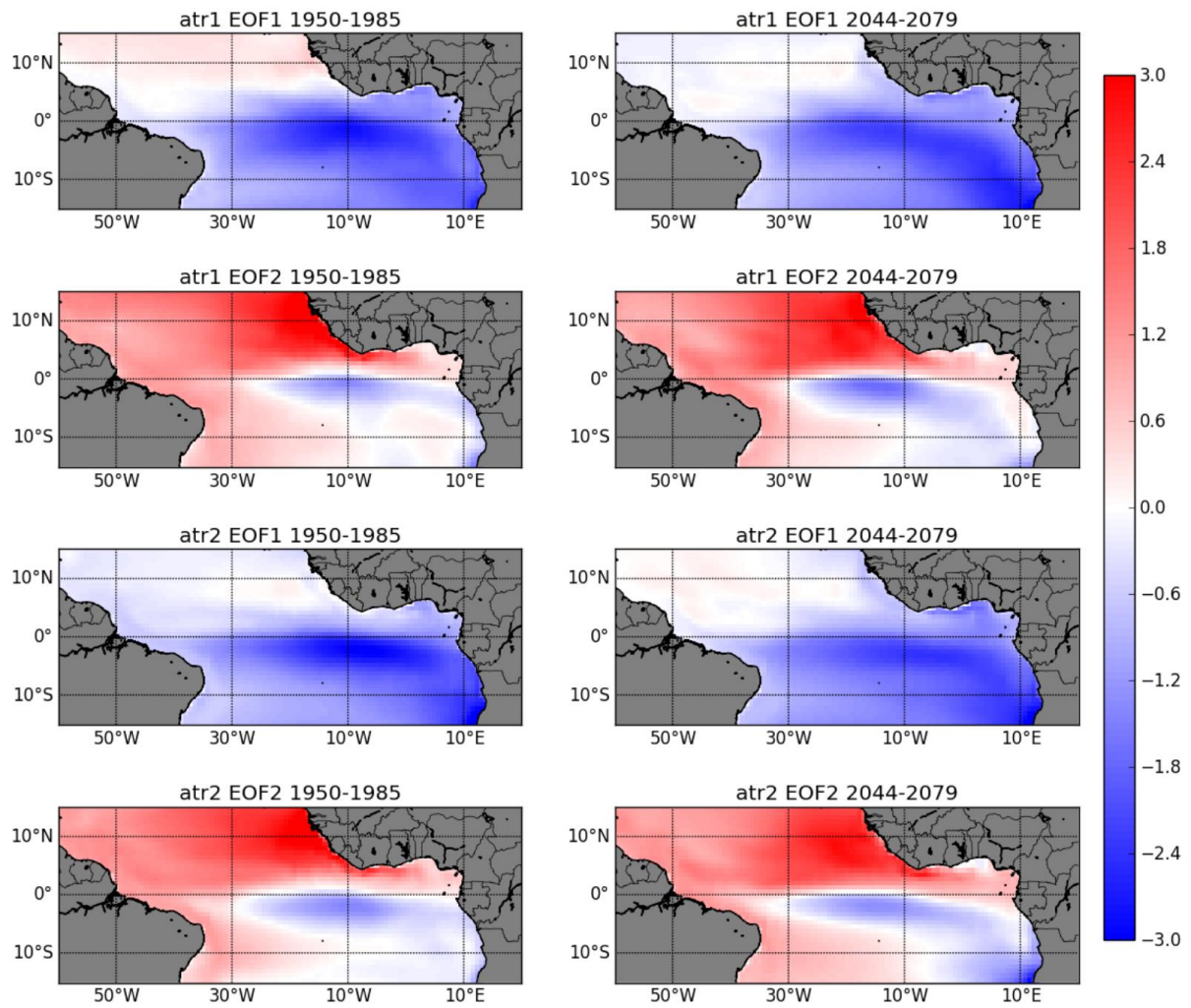


Figure 2.2: EOFs of SST for the two transient runs for a historic period (1950-1985, left column) and a period in the future (2044-2079).

Act1	Atr1	Atr2
Historic control run	Transient control run	Transient run with increased vertical mixing parameter rn_ediff

Table 1: Simulations performed with 3D EC-Earth

### 3. Simulated Tropical Atlantic variability in future climate projections with the new version of CNRM-CM model

Sanchez-Gomez E. (CERFACS); Voltaire A. (MF-CNRM)

In the previous deliverable D7.2 we documented the representation of Tropical Atlantic Variability (TAV) in the new version of the CNRM-CM coupled model developed by the MFCNRM/CERFACS modelling group (Toulouse, France). CNRM-CM6 will participate in the CMIP6 (Coupled Model Inter-comparison Phase 6) exercise through several MIPs. A detailed list of developments and modifications performed for the new model version, regarding the previous one (CNRM-CM5) was provided in D7.2 and several publications including the model design and performances are being prepared (Voldoire et al. in prep). Main results reported in D7.2 show an improvement of the simulated mean state. Though the impact on the variability is lower, the simulation of the equatorial variability is improved in CNRM-CM6 regarding to CNRM-CM5. As for D7.2, we use here a pre-cmip6 version of CNRM-CM6.

In this study, we report the changes of mean climate and TAV modes in the future climate simulated by the two versions of CNRM-CM. On this purpose, we analyse an historical and scenario (RCP85) experiments performed with the two model versions. The periods considered for each experiment is 1970-1999 for historical, and 2070-2099 for the climate projection (considering scenario RCP85). Unfortunately only one member (realisation) of historical and scenario are available for CNRM-CM6 so far, hence only one member will be used for CNRM-CM5.

The historical simulation with CNRM-CM6 has been run using new CMIP6 aerosol historical forcings. For the RCP8.5 scenario, that was originally designed relative to CMIP5 historical forcings, there is a potential inconsistency with the aerosol forcing used for CMIP5 scenarios and the new CMIP6 historical aerosol forcing. So as to limit this potential inconsistency, the CMIP6 aerosol pattern averaged over 1995-2004 has been scaled to the global mean aerosol optical depth from the RCP8.5 scenario.

As for D7.2, we conduct an Empirical Orthogonal Function (EOFs) analysis on the detrended monthly sea surface temperature (SST) anomalies to obtain the TAV modes. We focus here in spring (April-May-June (AMJ)), where the Atlantic Meridional Mode (AMM; Nobre and Shukla 1996) peaks, and in summer (July-August-September (JAS)), where the equatorial variability is maximum (i.e. Equatorial Mode (EM; Carton et al. 1996)). Although the TAV modes in both model versions were previously compared in D7.2, the modes obtained from the observational dataset HADISST are also shown in Figures 1 and 4 for AMJ and JAS respectively.

A-Regional mean climate change:

The sensitivity to CO<sub>2</sub> of the CNRM-CM6 version is largely increased relatively to CNRM-CM5. The average SST change in the tropics between 1970-1999 and 2070-2099 is **3,4K** in CNRM-CM6 whereas it was **2,4K** in CNRM-CM5. In the following we discuss the SST change pattern relatively to this mean tropical change.

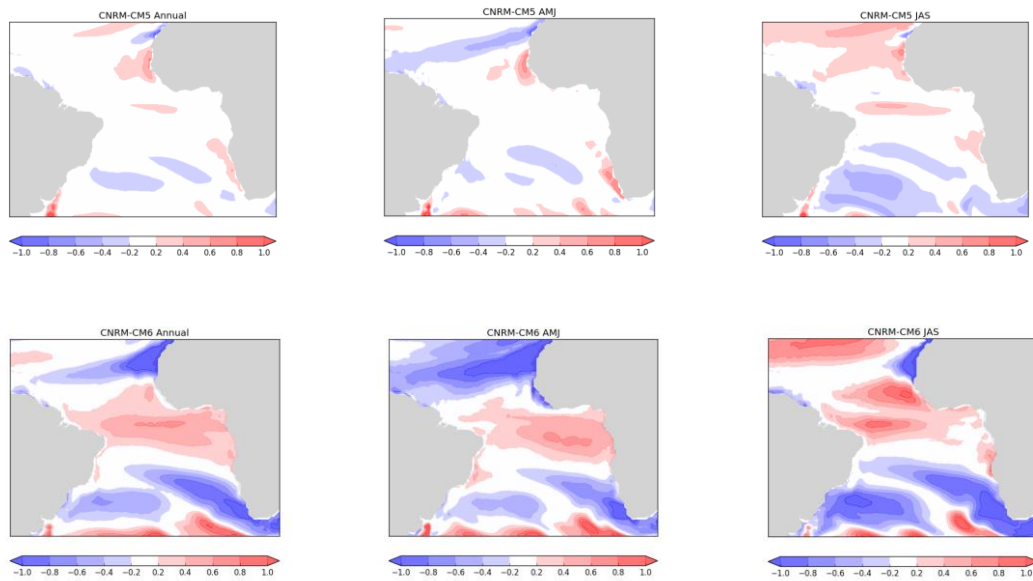


**Figure 3.1.** Annual mean, AMJ and JAS SST change relative to the tropical mean warming for CNRM-CM5 (top) and CNRM-CM6 (bottom) between the periods 1970-1999 and 2070-2099 (in K).

Even when subtracting the tropical mean climate change, the SST change pattern is much sharper in CNRM-CM6 compared to CNRM-CM5 (Fig. 3.1). The annual mean change in CNRM-CM6 is more intense over the Equator and weaker in the higher latitudes. The AMJ pattern is very similar to the annual mean pattern. In JAS, the northern tropics warming is more intense than the tropical mean warming as was the case for CNRM-CM5 although the intensification is higher than in CNRM-CM5.

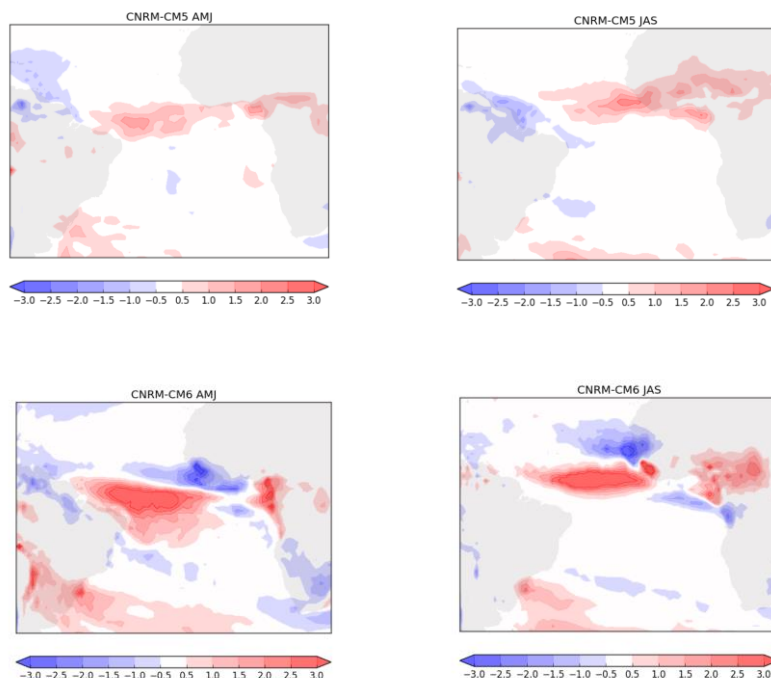
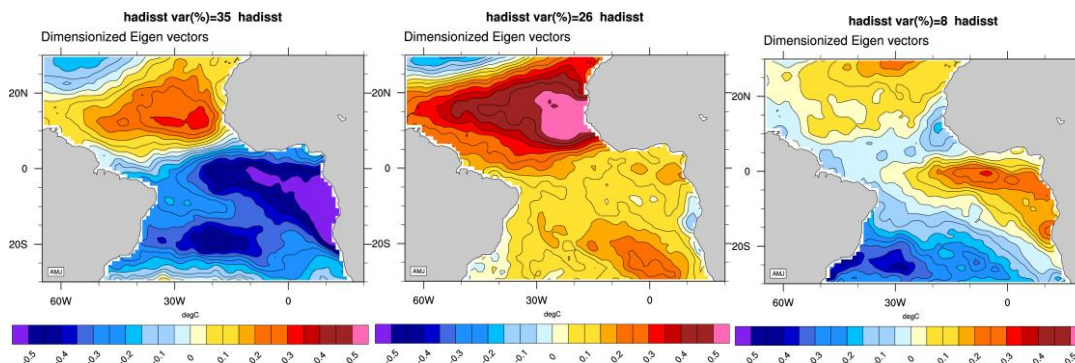


**Figure 3.2.** AMJ and JAS precipitation change for CNRM-CM5 (top) and CNRM-CM6 (bottom) between the periods 1970-1999 and 2070-2099 (in mm.d<sup>-1</sup>).

In CNRM-CM5, the impact of climate change on regional precipitation (Fig. 3.2) is mainly an increase in ITCZ precipitation, and a decrease of near Amazonian coast precipitation both in AMJ and JAS. In CNRM-CM6, the mean climate change is more complex: there is a dipole with decreased precipitation over the Equator in AMJ and an increase northward, this dipole moving northward in JAS. We may suspect a displacement of the ITCZ. Precipitation is increased over central Africa in JAS. As for CNRM-CM5, there is also drying near the Amazonian coast. In D7.2, it has been shown that the mean climate representation was improved in CNRM-CM6, and this clearly impacts the climate projections regionally. The processes associated to these changes have to be analysed in more detail to assess their reliability.

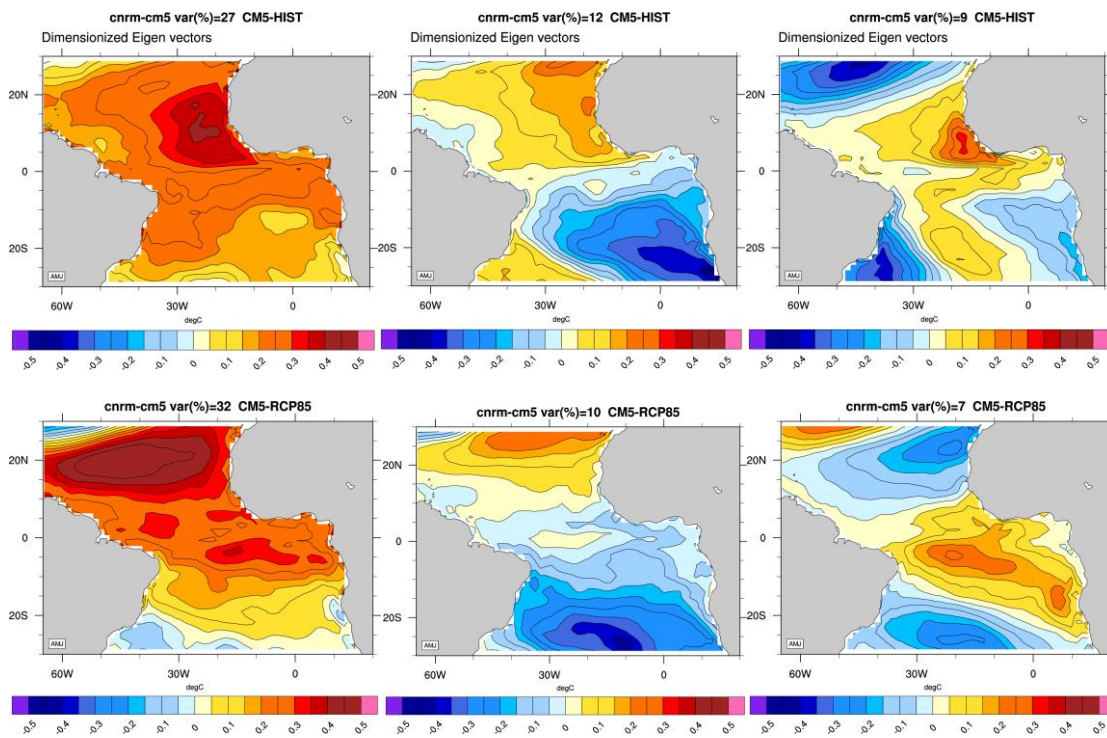
B- Analysis of spring TAV modes:

The 3 first TAV modes obtained from observations show a meridional dipole for the first mode, explaining 35% of the total variance, a second more homogeneous basin-wide pattern with a large centre of variability in the northeastern Tropical Atlantic (26%) and third pattern with centres on the eastern equatorial region and north and south Tropical Atlantic (8%) as shown in Fig.3.3. The first TAV mode for observations clearly corresponds to the AMM. The dipole-like structure for the first observational mode is not captured in CMRM-CM5 for the historical period (Fig.3.4). The latter exhibit a homogeneous pattern explaining 27% of the total variance. We observe that for the first mode in the RCP85 experiment (32% of the variance), the centre of maximum variability moves to the north Tropical Atlantic



**Figure 3.3.** SST anomalies associated to the first three TAV modes (units in degrees Celsius) in AMJ for ERAI for the period 1970-1999. The percentage of explained variance is indicated in on the top of each figure.

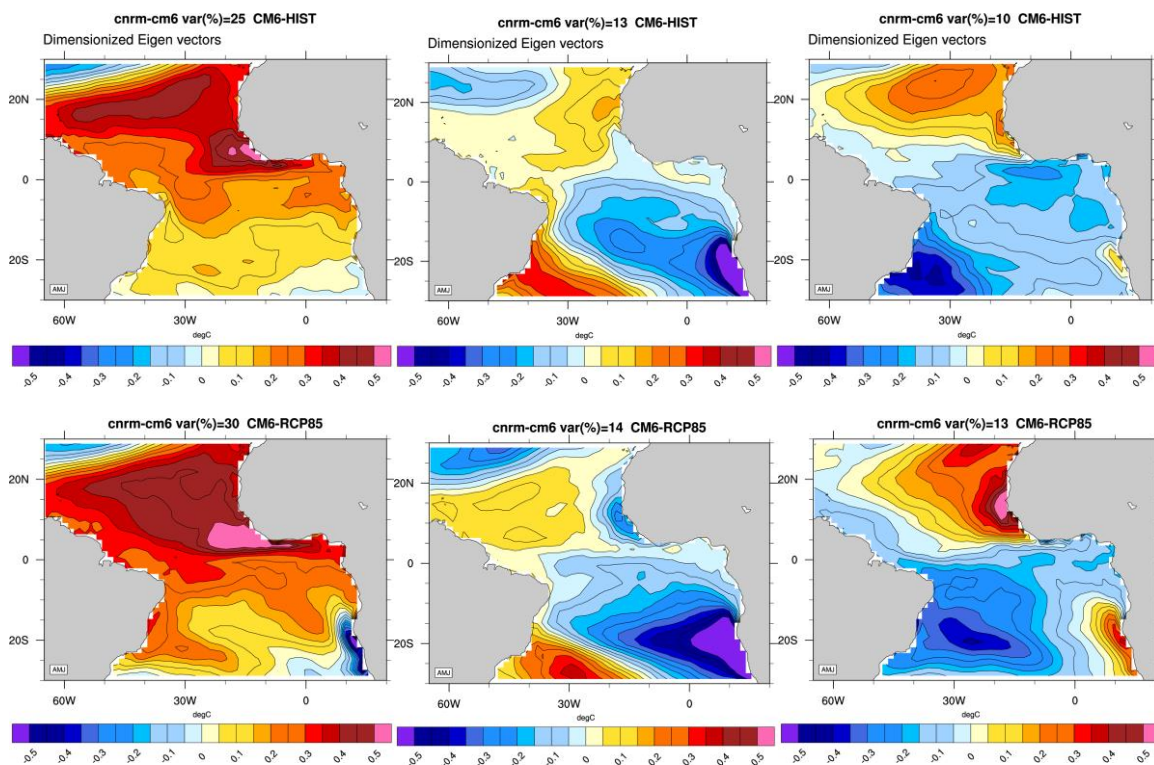
The second mode in CNRM-CM5 is more reminiscent of a dipole-like pattern, explaining 12 and 11 % of the total variance of the historical and RCP85 respectively. Once again the variability moves poleward in the scenario experiment.



**Figure 3.4. SST anomalies associated to the first three TAV modes (units in degrees Celsius) in AMJ for CNRM-CM5. (Top) Historical simulation (1970-1999); (bottom) rcp85 simulation (2070-2099). The percentage of explained variance is indicated in on the top of each figure.**

As seen in Fig.3.5, CNRM-CM6 fails also in simulating the AMM as the main structure of variability in boreal spring. As for CNRM-CM5, the first TAV is an homogeneous SST pattern whose spatial structure does not change that much in the future climate, but does the variance (25% to 30%). Interhemispheric SST gradients are not present either in the second TAV mode, which is more a dipole SST pattern in the Tropical South Atlantic. The third variability mode is more reminiscent of a north-south SST dipole, explaining 10 and 13% of the variance.

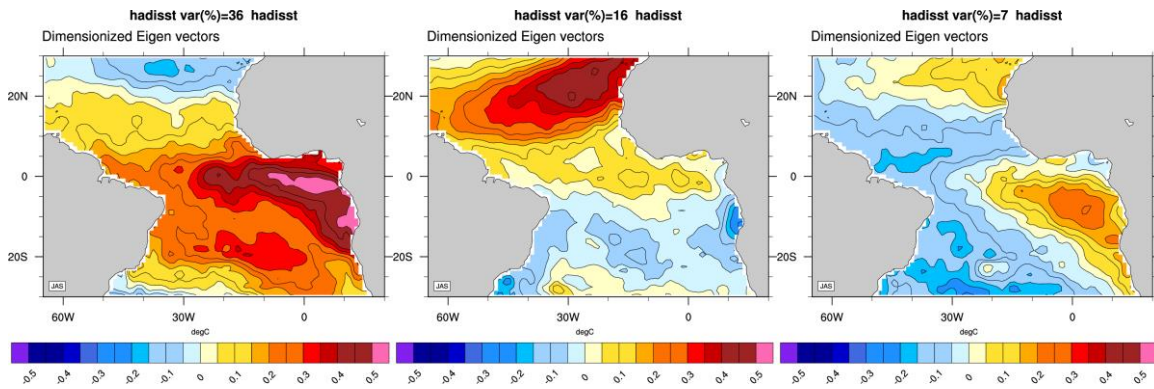
To conclude, even if there are deficiencies in representing the TAV modes in spring in the new model version (the reason explaining this need more investigation), it seems clear that TAV modes in CNRM-CM5 in spring are more sensitive to global warming (induced by the RCP85 forcing) than in CNRM-CM6.



**Figure 3.5.** SST anomalies associated to the first three TAV modes (units in degrees Celsius) in AMJ for CNRM-CM6 (PRE-CMIP6). (Top) Historical simulation (1970-1999); (bottom) rcp85 simulation (2070-2099). The percentage of explained variance is indicated in on the top of each figure.

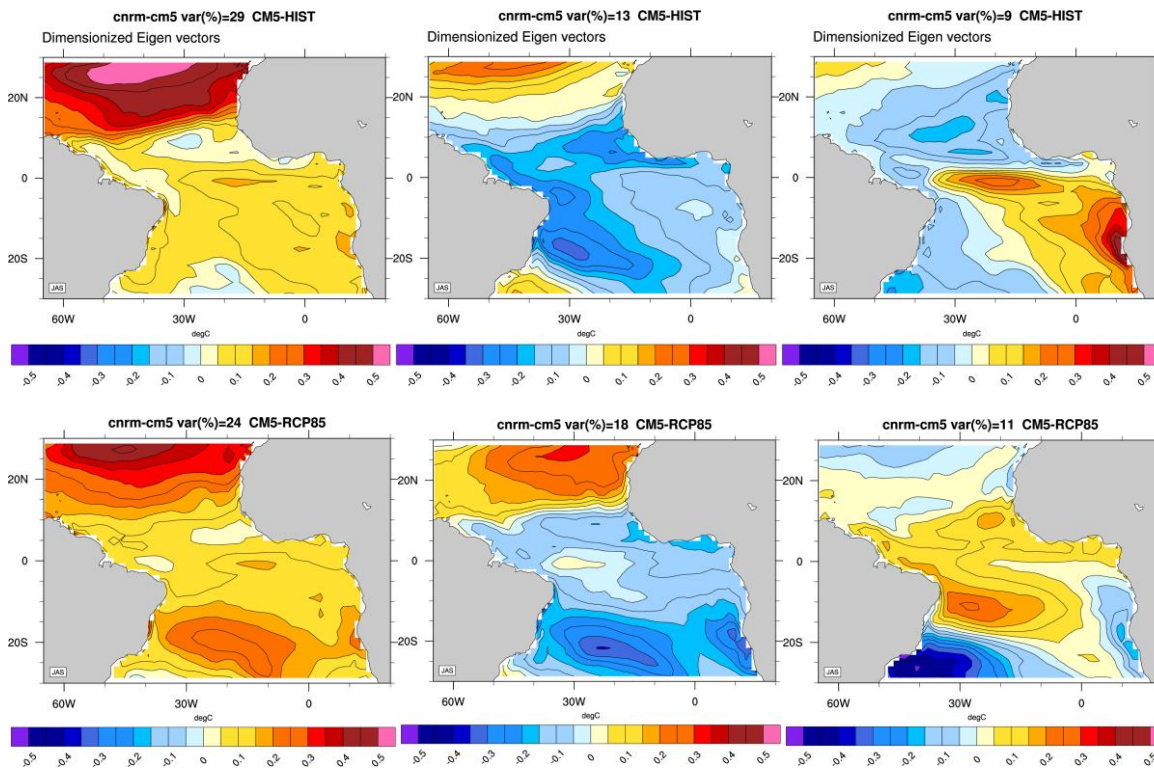
C- Analysis of summer TAV modes:

Figure 3.6 shows the SST anomalies associated to the first 3 TAV modes for HadISST observations in summer. The first mode is the well-known EM, explaining the 36% of the total explained variance, followed by a dipole SST inter-hemispheric gradient, weaker than the AMM (16%) and a tropical Atlantic tripole (7%). As shown in Fig.3.7, CNRM-CM5 fails to represent the EM as first model of TAV. Once again, the leading SST mode is a homogeneous SST pattern in historical and RCP85 explaining 29% and 24% of the explained variance respectively. The second mode for both historical and RCP85 is a dipole SST pattern, whose centres of action located differently in the Southern hemisphere part. The third mode is quite different between historical and scenario : in the historical is a tripole like SST pattern in the Tropical Atlantic and in the scenario is a south Atlantic SST dipole located in the western part of the basin.



**Figure 3.6.** SST anomalies associated to the first three TAV modes (units in degrees Celsius) in JAS for ERAI for the period 1970-1999. The percentage of explained variance is indicated in on the top of each figure.

Figure 3.8 shows the historical and RCP85 TAV modes for CNRM-CM6. The first mode is again and homogeneous basin-wide SST anomaly pattern, which maximum of variability in the north for the present climate conditions and south of equator, near the Brazilian coast, for future climate conditions. These modes approximatively represent ~22% of the variance in both cases, which is clearly underestimated regarding observations.



**Figure 3.7.** SST anomalies associated to the first three TAV modes (units in degrees Celsius) in JAS for CNRM-CM5. (Top) Historical simulation (1970-1999); (bottom) rcp85 simulation (2070-2099). The percentage of explained variance is indicated in on the top of each figure.

The second TAV mode in CNRM-CM6 is quite similar to the observed one and does change significantly between historical and RCP85 conditions, except for the southern boundary of the

domain. The explained variance increases in the RCP85 (20%) respect to the historical one (15%), whose value is very close to the observed one (16%). The third mode of CNRM-CM6 is quite well simulated and is unchangeable between historical and RCP85.

Similar conclusions can be drawn here for the summer variability, TAV modes simulated by CNRM-CM6 are less different between historical and scenario simulations than the ones simulated by CNRM-CM5. The reasons for that need to be investigated, since many mechanisms can be at play: changes in the mean state of the Tropical Atlantic climate (both in the ocean and atmosphere), changes in the teleconnections between the Pacific, the North Atlantic and the South Atlantic.

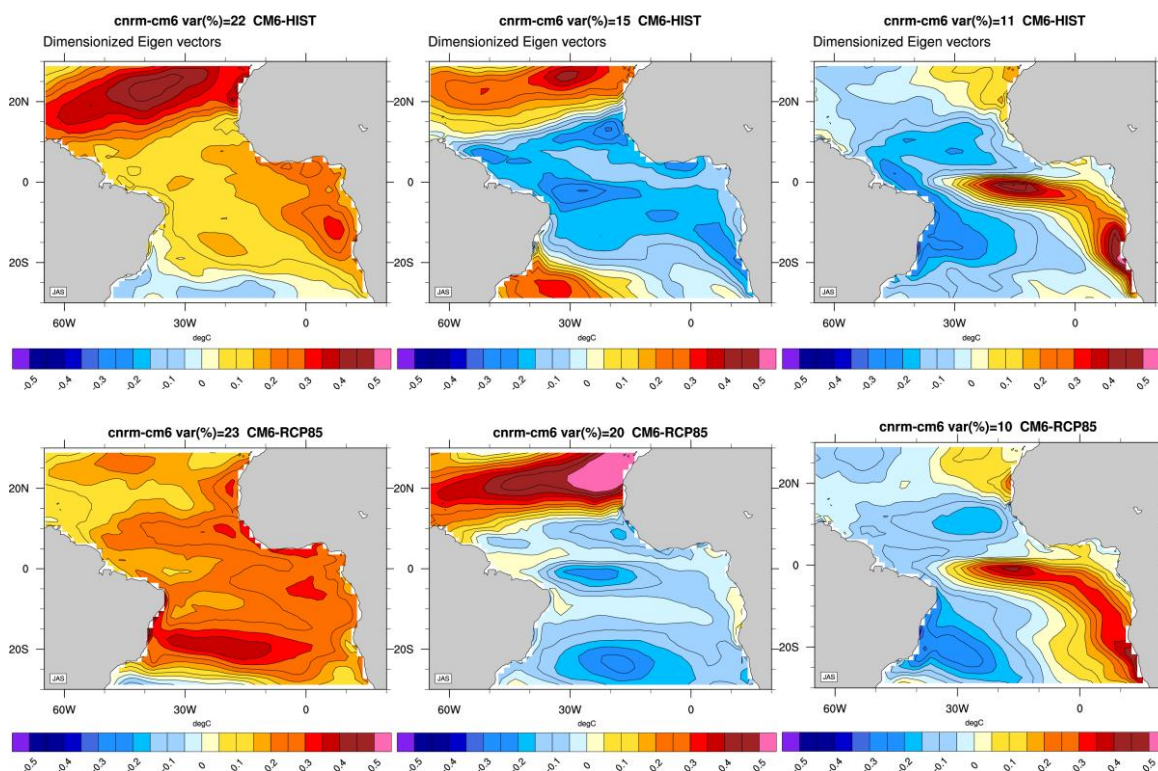


**Figure 3.8.** SST anomalies associated to the first three TAV modes (units in degrees Celsius) in JAS for CNRM-CM6 (PRE-CMIP6). (Top) Historical simulation (1970-1999); (bottom) rcp85 simulation (2070-2099). The percentage of explained variance is indicated in on the top of each figure.

#### 4. Inter-basin Teleconnection under warm climate

Martín-Rey M.(CERFACS); Cassou C.(CERFACS); Sanchez-Gómez E. (CERFACS)

El Niño-Southern Oscillation (ENSO) is the leading air-sea coupled mode of inter-annual variability in the tropical Pacific with worldwide climate impacts. Recent studies have reported that the Global Warming (GW), induced by GHG external forcing, could affect the ENSO phenomena in a long-term future climate (i.e. the frequency, intensity, spatial pattern) and consequently the ENSO teleconnections and impacts. In addition, the role of the internal climate variability seems to be crucial to amplify or attenuate the GW effect in the near-term horizon.

In the present study, we use a pacemaker protocol in a perfect model framework by using the coupled model CNRM-CM5 to disentangle the influence of the mean background state in ENSO teleconnections. This experimental design, based on Kosaka and Xie (2013), has considered a set of 30 years representative of the CNRM-CM5 model ENSO flavour and close to observations (ENSO diversity in timing, amplitude, spatial properties) from the pi-control run. Ensemble simulations have been performed restoring through flux formulation towards the 30-yr selected monthly anomalies only over the Eastern Pacific using two different mean states: piControl and RCP85 (Drouard and Cassou 2018). The initial conditions are taken randomly in piControl or RCP85 respectively. Hereinafter, we denote these simulations as ENSOCPI and ENSOCF respectively. These experiments allow us to isolate the impact of the background state in the modification of ENSO teleconnection, because by construction, they share the same ENSO events.

We have focused our study in the alteration of the ENSO-Tropical Atlantic teleconnection. Under a warmer climate (ENSO CF), the connection between the tropical Atlantic surface and subsurface variables is stronger, showing significant positive correlations between the sea surface temperature (SST), sea surface height (SSH) and mixed layer (MLD), especially during boreal spring and summer seasons (Fig. 4.1a-d). It contrasts with weaker and not significant (even negative) correlation in ENSOCPI simulations. These results could suggest the existence of more dynamical mechanisms in ENSOCF in the tropical Atlantic basin.

The global background state has changed in ENSOCF respect to ENSOCPI, showing warmer conditions (up to 4°C) in the tropics, associated with a deeper mixed layer and elevation of the SSH. Consequently, the Subtropical Highs Pressure Systems are weakened, reducing the trade winds along the tropical band. The ITCZ is displaced southward in a warmer climate during boreal winter and spring, while the convection is enhanced north-equator during summer months (Fig. 4.1e-f). Furthermore, the mean Walker circulation is debilitated in the tropical Pacific and Atlantic basins (Fig. 4.1g-h).

Regarding the ENSO-TA teleconnection, under a warmer scenario the ENSO-forced diabatic source along the equator suffers an eastward shift, causing an eastward displacement of the centres of action in the North Pacific (Drouard and Cassou 2018) and a stronger NAO-like pattern over North

Atlantic. It originates a stronger reduction of the trades in the northern part of the basin during boreal winter and spring (Fig. 4.2a-d). Furthermore, the link between ENSO and TA through the alteration of the Walker circulation is suppressed under a warmer climate, reducing the sea level pressure and wind forcing over the equatorial Atlantic (Fig. 4.2a-d).

Interestingly, in ENSOCF simulation, the rotational of the wind field is able to excite an oceanic Rossby wave north of equator that is reflected in the western boundary and propagates as an equatorial Kelvin wave from boreal spring to summer (Fig. 4.2e-f). This mechanism, in agreement with the studies of Foltz and McPhaden (2010) and Martín-Rey and Lazar (2018), is not present in the ENSOCPI experiment. Therefore, we conclude that the ENSO-TA teleconnection is much more prominent in a warmer climate due to an intensified ENSO atmospheric signal and more active ocean dynamics in the TA. Our results highlight the importance of the background state in modulating the ENSO teleconnections in a future scenario (Martín-Rey et al. 2018).

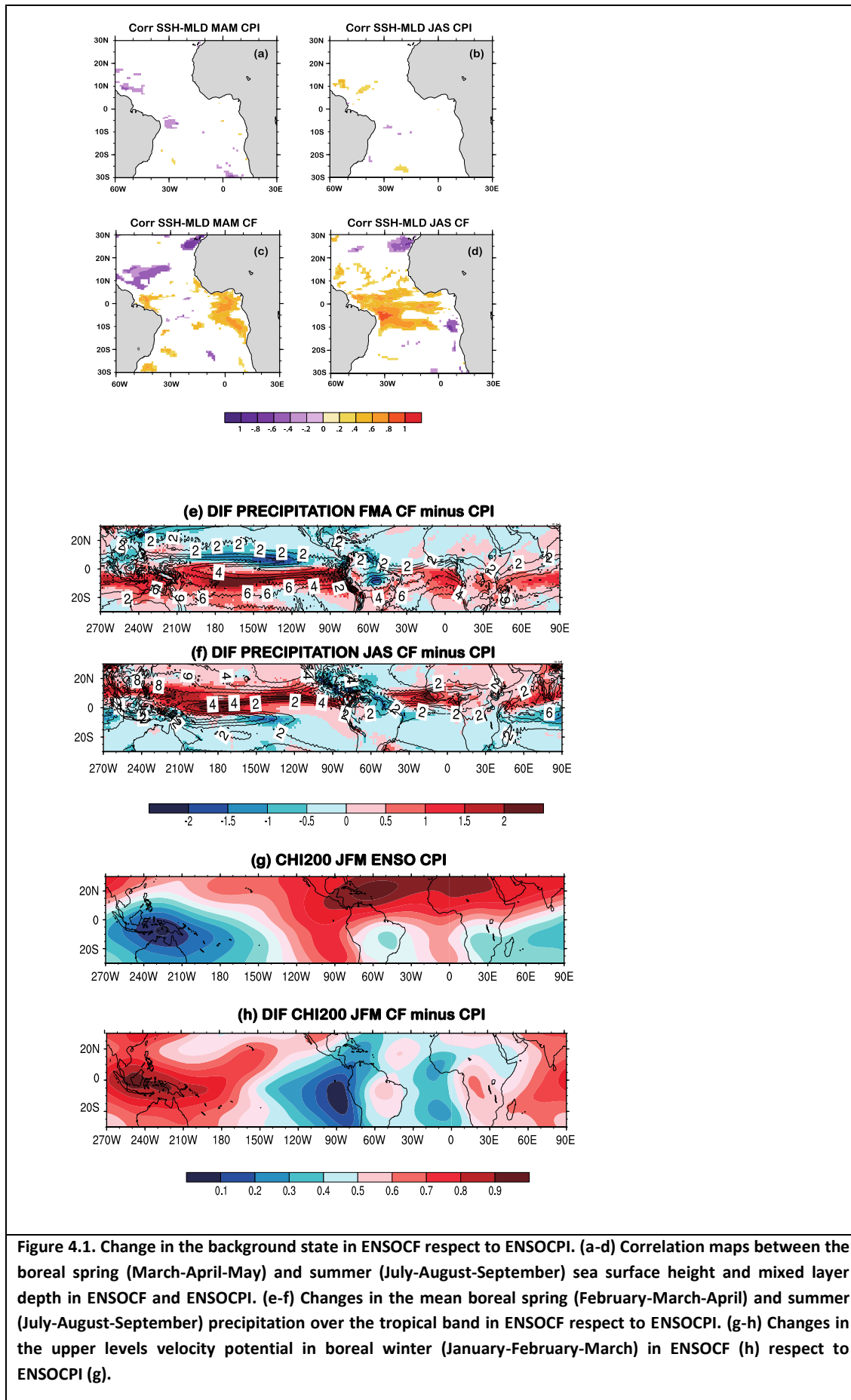


**Figure 4.1.** Change in the background state in ENSOCF respect to ENSOCPI. (a-d) Correlation maps between the boreal spring (March-April-May) and summer (July-August-September) sea surface height and mixed layer depth in ENSOCF and ENSOCPI. (e-f) Changes in the mean boreal spring (February-March-April) and summer (July-August-September) precipitation over the tropical band in ENSOCF respect to ENSOCPI. (g-h) Changes in the upper levels velocity potential in boreal winter (January-February-March) in ENSOCF (h) respect to ENSOCPI (g).

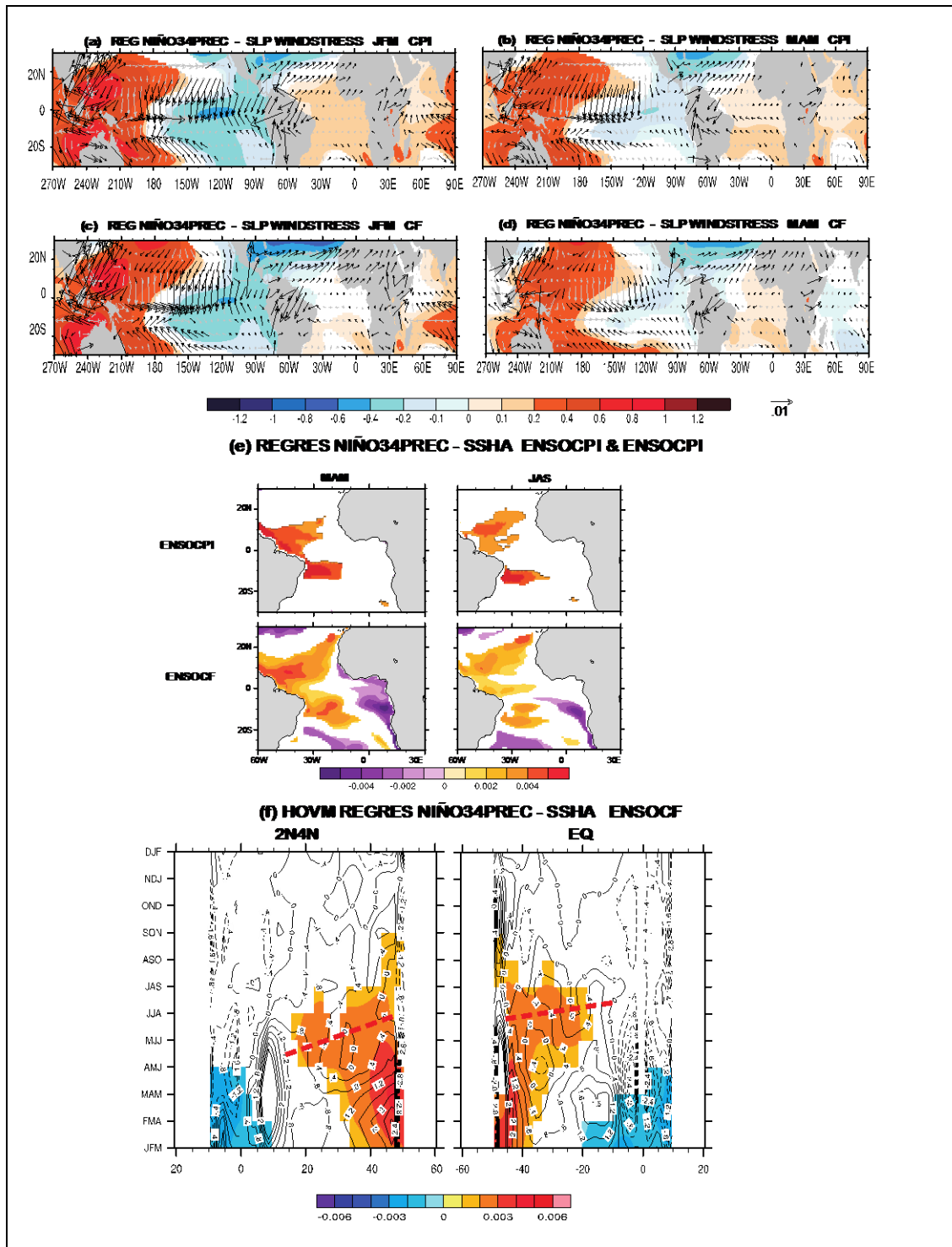


Figure 4.2. (a-d) Regression of the anomalous boreal winter (January-February-March) and spring (March-April-May) SLP (shaded) and wind stress (vectors) over boreal winter (DJF) Niño34 precipitation anomalies in ENSOCPI and ENSOCF simulations. (e) Regression of the anomalous boreal spring (March-April-May) and summer (July-August-September) SSH (shaded) over boreal winter (DJF) Niño34 precipitation anomalies in ENSOCPI and ENSOCF simulations. (f) Time-longitud diagrams along 20°N and EQ of the regression of the anomalous SSH (shaded) over boreal winter (DJF) Niño34 precipitation anomalies in ENSOCF simulation. The rotational of the wind stress is shown in contours. Shaded areas and black vectors are statistically significant at 95% confidence level according to a Bootstrap test.

**References (in bold are PREFACE articles)**

Carton, J. A., and B. Huang, 1994: Warm Events in the Tropical Atlantic. *J. Phys. Ocea.*, **24**, 888-903.

Drouard, M and Cassou C (2018) Sensitivity of ENSO Teleconnection to mean background states: pre-industrial vs late XX1st century under RCP85 scenario (to be submitted).

Foltz, G. R., & McPhaden, M. J. (2010). Interaction between the Atlantic meridional and Niño modes. *Geophysical Research Letters*, *37*(18).

**Hartung, K., G. Svensson, H. Struthers, A.-L. Deppenmeier, W. Hazeleger, “An EC-Earth coupled atmosphere-ocean Single Column Model (AOSCM) for studying marine and polar processes”, in preparation**

Kosaka, Y., & Xie, S. P. (2013). Recent global-warming hiatus tied to equatorial Pacific surface cooling. *Nature*, *501*(7467), 403-407.

**Koseki S. and N. Keenlyside. On the tropical Atlantic variability in a CGCM. In preparation.**

**Martín-Rey M, C Cassou and E Sánchez-Gómez (2018) Role of the ocean dynamics in ENSO-tropical Atlantic teleconnection under warmer climate (in preparation)**

**Martín-Rey M and Lazar A (2018), Is the boreal spring Tropical Atlantic SST variability a precursor for the Equatorial Mode? (to be submitted)**

Nobre, P., and J. Shukla, 1996: Variations in sea surface temperatura, wind stress, and rainfall over the tropical Atlantic and South America. *J. Climate*, **9**, 2464-2479

**Pillar H. R., M. Jochum, and R. Nuterman. Impacts of Oceanic Inertial Mixing on Modelled Seasonal to Decadal Climate Variability. In preparation.**

Ruiz-Barradas, A., Carton, J.A., Nigam, S., 2000 : Structure of interannual-to-decadal climate variability in the tropical atlantic sector. *Am. Met. Soc.* 13

**Toniazzo T., and S. Koseki. A methodology of anomaly coupling for climate simulation. To be submitted to *Journal of Advances in Modeling Earth System*.**

**Voldoire A. and co-autors, The CNRM-CM6.1 global climate model : Description and basic evaluation, in preparation.**

Xie S-P and Philander SGH, 1994 : A coupled ocean-atmosphere model of relevance to the ITCZ in the eastern Pacific *Tellus* 46A 340-350

Xie S-P and Carton J A, 2004 : Tropical Atlantic variability: Patterns, mechanisms, and impacts. In *Earth Climate: The Ocean-Atmosphere Interaction* Wang C, Xie S-P and Carton J A (eds.), AGU Geophysical Monograph 147 121-142